

ENDOCRANIAL ANATOMY OF THE CERATOPSIDAN DINOSAUR *PSITTACOSAURUS LUJIATUNENSIS* AND ITS BEARING ON SENSORY AND LOCOMOTOR ABILITIES

Rina SAKAGAMI¹, Soichiro KAWABE^{2,3}, Soki HATTORI^{2,3}, Wenjie ZHENG⁴ and Xingsheng JIN⁴

¹Department of Bioscience and Biotechnology, Fukui Prefectural University, 4-1-1 Matsuoka Kenjojima, Eiheiji, Fukui 910-1195, Japan

²Institute of Dinosaur Research, Fukui Prefectural University, 4-1-1 Matsuoka Kenjojima, Eiheiji, Fukui 910-1195, Japan

³Fukui Prefectural Dinosaur Museum, 51-11 Terao, Muroko, Katsuyama, Fukui 911-8601, Japan

⁴Zhejiang Museum of Natural History, Hangzhou, Zhejiang 310014, People's Republic of China

ABSTRACT

Psittacosaurus is one of the dinosaurs with the highest number of skull morphologies analyzed. *Psittacosaurus lujiatunensis*, in particular, is rich in morphological variation. Nevertheless, the intracranial neuroanatomy has not yet been thoroughly analyzed. Hence, in order to understand the neuroanatomy of the ceratopsian *P. lujiatunensis*, two well-preserved skulls of this species were analyzed using computed tomography (CT). Three-dimensional digital endocasts of the cranial cavities and bony labyrinths were generated. They show that the cerebellar flocculi, which had not previously been reported in *P. lujiatunensis*, is large for a ceratopsian. The enlarged cerebellar flocculi and well-developed semicircular canals support the hypothesis that *P. lujiatunensis* had better gaze stability and balance than other ceratopsians. The olfactory bulbs of *P. lujiatunensis* were relatively large compared to those of other dinosaurs, suggesting that *P. lujiatunensis* possibly had a keen sense of smell. The cochlea was short compared to that of the other dinosaurs, indicating that the *P. lujiatunensis* heard better at higher frequencies. This study provides insights into the ecology and habits of *P. lujiatunensis*. The re-evaluation of the neuroanatomy of dinosaurs using high-resolution CT analyses on well-preserved fossil specimens is crucial for a better understanding of their ecology.

Key words: digital endocast, endosseous labyrinth, *Psittacosaurus lujiatunensis*

坂上莉奈・河部壮一郎・服部創紀・鄭文傑・金幸生 (2023) 角竜類 *Psittacosaurus lujiatunensis* の脳・内耳形態と知覚・運動機能との関係。福井県立恐竜博物館紀要 22: 1–12

Psittacosaurus は、最も多くの頭骨形態が解析されている恐竜の一つで、特に *Psittacosaurus lujiatunensis* は、形態的バリエーションが豊富である。一方で、その頭骨内部の神経解剖学解析ははまだ十分な精度で行われているとは言えない。そこで、2 個体の保存状態のよい *P. lujiatunensis* の頭骨を CT 撮影し、頭蓋腔及び骨迷路のデジタルエンドキャストを作成した。これらのエンドキャストの解析から、これまで角竜類では報告されていなかった発達した小脳片葉が *P. lujiatunensis* に見られることが初めて確認された。小脳片葉の発達は視線の安定性に関係することから、*P. lujiatunensis* は他の角竜類よりも視線の安定性や俊敏性に優れていた可能性がある。また、*P. lujiatunensis* の嗅球は比較的用いた恐竜類の中では比較的大きく、鋭い嗅覚を持っていたことが分かった。さらに、*P. lujiatunensis* の蝸牛管は比較した恐竜類の中では短く、比較的高い周波数を聞くことに適していたことが示された。このように、本研究は *Psittacosaurus* の生態や習性に関する知見を改めて得るものとなり、保存状態の良い化石標本を用いた高解像度 CT 解析による恐竜の神経解剖学の再評価は、恐竜の詳細な生態を解明するためにも重要であることを示すものとなった。

INTRODUCTION

Several previous studies have investigated the neurosensory function among ceratopsian dinosaurs (e.g., Brown, 1914; Hopson, 1979; Forster, 1996; Zhou et al.,

2007; Witmer and Ridgely, 2008). Among basal non-neoceratopsian ceratopsians, *Psittacosaurus* has been the subject of neuroanatomical works in which multiple digital cranial endocasts were produced through computed tomography (CT) analyses (Zhou et al., 2007; Bullar et al., 2019; Napoli et al., 2019). This is probably because this species is one of the most abundant dinosaurs for which cranial specimens can be found. Zhou et al. (2007) examined three endocasts of *Psittacosaurus lujiatunensis*. They found that *P. lujiatunensis* had large olfactory bulbs and optic

Received September 22, 2022. Accepted May 26, 2023.

Corresponding author—Soichiro KAWABE

E-mail: kawabe_soichiro@yahoo.co.jp

lobes. They also stated that the encephalization quotients were higher than that of the theropod dinosaur *Tyrannosaurus*. The results of Zhou et al. (2007) suggested that *Psittacosaurus* likely exhibited complex behavior, had a keen sense of smell, and had acute vision. In addition, Zhou et al. (2007) showed that *Psittacosaurus* possessed relatively taller anterior semicircular canals than *Protoceratops* and more derived ceratopsids, which suggests that this animal could have been agile when trying to escape from predators. Bullar et al. (2019) compared the inner ear morphology of three individuals of *Psittacosaurus lujiatunensis* at different ontogenetic stages based on digital endocasts and discussed changes in head postures through development. Napoli et al. (2019) described the cranial endocast of *Psittacosaurus amitabha*. They mentioned that a slightly ventrally-oriented head posture was probable because the lateral semicircular canal is slightly anterodorsally tilted.

Those studies provided valuable insights into the neuroanatomy of *Psittacosaurus*. However, the results of the CT analyses may have been impacted by the state of preservation of the specimens. In addition, with the enhancement of CT techniques and imaging, previously overlooked anatomical features may now be detected. In this study, we analyzed two well-preserved specimens of *P. lujiatunensis* and conducted quantitative comparisons of several endocranial anatomical features with other dinosaurs to improve the understanding of the neuroanatomy and paleoecology of *P. lujiatunensis*.

MATERIALS AND METHODS

Specimens and CT scanning

The specimens analyzed in this study include two skulls of *Psittacosaurus lujiatunensis* (ZMNH M12414 and ZMNH M12423) recovered from the Lower Cretaceous (Barremian) (Li et al., 2022) Lujiatun Beds of Yixian Formation in Liaoning, China. They are housed in the Zhejiang Museum of Natural History (ZMNH), Zhejiang, China. Threedimensional (3D) geometric morphometric analyses suggested that the three psittacosaurid species from the Lujiatun Beds (*Hongshanosaurus houi*, *P. lujiatunensis*, and *Psittacosaurus major*) are actually taphomorphotypes of *P. lujiatunensis* (Hedrick and Dodson, 2013). We follow Hedrick and Dodson (2013) and assign the specimens to *P. lujiatunensis*. The specimens were CT scanned with a micro-focus X-ray CT XT H 320 (Nikon Solutions Co., Ltd.) at the College of Civil Engineering and Architecture, Zhejiang University (Hangzhou, Zhejiang, China) (see Table 1 for scan parameters). We subsequently prepared the digital endocasts of the neurocranial cavities and bony labyrinths from the acquired CT images using the software Amira (v 2019.3, Thermo Fisher Scientific; Waltham, MA, USA). Corfield et al. (2008) and Balanoff et al. (2016) provided detailed methods to prepare and examine the endocast models.

TABLE 1. Specimens used for this study and the relevant scan parameters.

Specimen #	Energy (kV)	Amps (μ A)	Resolution (μ m)
ZMNH M12414	300	280	90
ZMNH M12423	280	200	70

Generally, reptile brains – including presumably those of non-theropod dinosaurs – do not fill the endocranial cavity (Hopson, 1979). Furthermore, it is known that the distance between the brain and the cranial bones forming the cranial cavity, i.e., the shape difference between the cranial endocast and the actual brain, increases with development among nonavian archosaurs (Jirak and Janacek, 2017). Therefore, the endocasts do not provide an accurate picture of the brain morphology in these animals. Particularly, the posterior part of an endocast tends to appear larger than that of the actual brain in reptiles (Hopson, 1979; Watanabe et al., 2019). Despite these limitations, endocasts still provide a premier source of information on brain morphology in extinct species.

Measurements

To assess the olfactory bulb size of *P. lujiatunensis*, the ratio of the greatest diameter of the olfactory bulb to the greatest diameter of the cerebral hemispheres (i.e., olfactory ratio) was measured in the digital brain endocast of ZMNH M12414. Then, the common logarithm of the ratio was taken following Zelenitsky et al. (2009). Next, the ratio must be standardized to the log₁₀ body mass to compare the log₁₀ olfactory ratio with those in other dinosaurs.

The ontogenetic stage for each specimen was estimated by using the following regression equation established by Zhao et al. (2014), where X is the age in years, and Y is the skull length (from the posterior end of the occipital condyle to the anterior end of the rostrum) in mm:

$$Y = 15.8 X + 32.2$$

Subsequently, the body mass was calculated following Erickson et al. (2009), where the body mass is in kg and the age in years:

$$\text{body mass} = 37.38 \times \exp(0.55 \times \text{age}) / (37.38 + (\exp(0.55 \times \text{age}) - 1))$$

To assess the degree of development of the semicircular canals of *P. lujiatunensis*, the ratio of the height of the anterior semicircular canal (ASC) to its external diameter and the ratio of the total height of the posterior semicircular canal (PSC) to the height of the PSC below the plane of the lateral semicircular canal were calculated for ZMNH M12414 and M12423, following Domínguez Alonso et al. (2004) (Fig. 1; Table 2). Then, both ratios were compared with the results of Sakagami and Kawabe (2020) (Table 3).

The endosseous cochlear duct length (CL) for *P. lujiatunensis* was measured to estimate the best frequency of hearing and the hearing limit. The best frequency of hearing

TABLE 2. Measurements and calculated values used in this study.

Specimen #	Olfactory ratio (%)	Body mass (kg)	Relative ASC height	Relative PSC height	Endosseous cochlear length (mm)	Best frequency of hearing (Hz)
ZMNH M12414	57.48	18.4	1.353	0.416	5.07	2479
ZMNH M12423	-	9.1	1.381	0.428	4.33	2804

Relative ASC height, height of the anterior semicircular canal/external diameter of anterior semicircular canal; Relative PSC height, height from the base of the posterior semicircular canal to the plane of the lateral semicircular canal/height of the posterior semicircular canal.

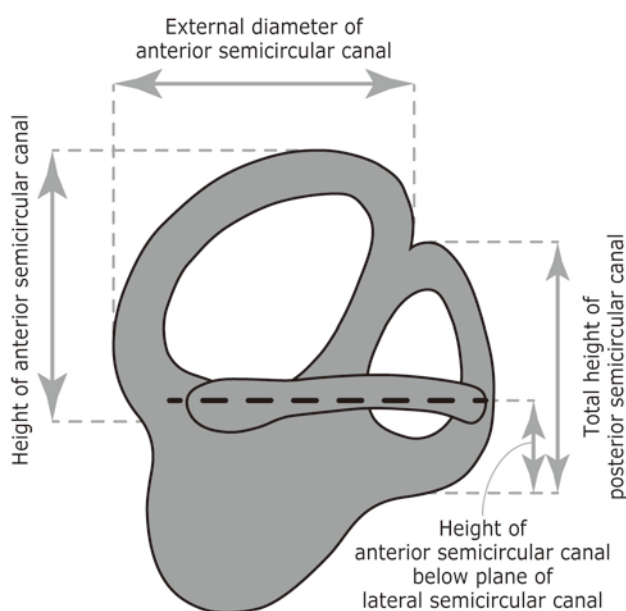


FIGURE 1. Measurement points for the endosseous labyrinth.

was calculated by the following regression equation proposed by Gleich et al. (2005), where X is the basilar papilla length, and Y is the best frequency of hearing:

$$Y = 5.7705 e^{-0.25X}$$

The basilar papilla lengths were calculated from the CL, based on the estimation of Gleich et al. (2005) that the basilar papilla length corresponds to two-thirds of the CL. The hearing limit was then determined following the regression equation by Gleich et al. (2005), in which X is the best frequency of hearing and Y is the highest frequency of hearing:

$$Y = 1.8436 X + 1.0426$$

Finally, the best and highest frequencies of hearing for *P.*

lujiatunensis were compared with those in the other taxa treated by Sakagami and Kawabe (2020) and Knoll et al. (2021) (Table 3).

RESULTS

ZMNH M12414 (Fig. 2) is well-preserved. In contrast, ZMNH M12423 (Fig. 3) appears to have suffered compressive deformation from dorsoventral forces approximately in the middle of the skull. A large dorsoventral crack extends through the anterior end of the left orbit and the right lateral end of the occiput. However, these deformation and crack do not significantly affect the area around the braincase. Based on the skull length of 134.6 mm, the ontogenetic stage and body mass of ZMNH M12414 were estimated to be six years and 18.4 kg. The skull length of ZMNH M12423 is 102.7 mm, from which the age and body mass were estimated as four years and 9.1 kg. The olfactory bulb of ZMNH M12423 could not be reconstructed due to the crack (Fig. 3), whereas that of ZMNH M12414 was reconstructed successfully (Fig. 2). In dorsal view, the olfactory bulb of ZMNH M12414 bifurcates to form an angle of approximately 17° with the midline anterior to the olfactory tract. The olfactory tract extends along the ventral surface of the frontals and gradually transitions to the cerebrum posteriorly (Fig. 2). The olfactory ratio was 0.57 (Table 2).

The cerebral shapes in ZMNH M12414 and M12423 resemble those of *Psittacosaurus lujiatunensis* (Zhou et al., 2007) and *Psittacosaurus amitabha* (Napoli et al., 2019). Their relative sizes are smaller than those of coelurosaurian theropods and hadrosaurid ornithopods (Evans et al., 2009; Witmer and Ridgely, 2009; Balanoff et al., 2018). Posterior to the cerebrum, the dorsal part of the hindbrain expands posterodorsally in each specimen (Figs. 2 and 3), supposedly due to dural sinus, as seen in *P. lujiatunensis* and *P. amitabha* (Zhou et al., 2007; Napoli et al., 2019). The optic lobe is expanded laterally in ZMNH M12414 (Fig. 4), while it is unobservable in ZMNH M12423, probably due to the taphonomic dorsoventral compression. The lateral expansion of the optic lobe is also recognized as a bulbous protrusion

TABLE 3. Proportions of the endosseous labyrinth and estimated hearing frequencies of selected dinosaurs.

	Specimen #	Relative ASC height	Relative PSC height	Endosseous cochlear length (mm)	Best frequency of hearing (kHz)	High frequency hearing limit (kHz)	References
<i>Psittacosaurus lujiatunensis</i>	IVPP V15451	1.286	0.426	-	-	-	Bullar et al. (2019)
<i>Psittacosaurus lujiatunensis</i>	IVPP V12617	1.237	0.371	-	-	-	Bullar et al. (2019)
<i>Psittacosaurus lujiatunensis</i>	PKUP V1054	1.3	0.235	-	-	-	Zhou et al. (2007)
<i>Protoceratops grangeri</i>	AMNH 6466	1.5	0.367	-	-	-	Hopson (1979)
<i>Pachyrhinosau- rus lakustai</i>	TMP 1989.55.1243	0.938	0.24	15.2	0.458	1.887	Witmer and Ridgely (2008)
<i>Anchiceratops ornatus</i>	AMNH 5259	1	0.25	-	-	-	Brown (1914)
<i>Triceratops</i> sp.	FPDM-V-9677	0.863	0.328	-	-	-	Sakagami and Kawabe (2020)
<i>Triceratops</i> sp.	FPDM-V-9775	0.85	0.292	17.95	0.29	1.577	Sakagami and Kawabe (2020)
<i>Lambeosaurus sp.</i>	ROM 758	-	-	9.2	1.245	3.339	Evans et al. (2009)
<i>Hypacrosauru- s altispinus</i>	ROM 702	-	-	16.7	0.357	1.7	Evans et al. (2009)
<i>Corythosaurus sp.</i>	ROM 759	-	-	11.9	0.794	2.507	Evans et al. (2009)
<i>Corythosaurus sp.</i>	CMN 34825	-	-	12.3	0.743	2.412	Evans et al. (2009)
<i>Proa- valdearinnoen- sis</i>	MAP AR-1- 2012	-	-	10	0.401	1.782	Knoll et al. (2021)
<i>Kunbarrasaur- us ieveri</i>	QM F18101	-	-	24.3	0.101	1.228	Leahey et al. (2015)
<i>Pawpawsaurus campbelli</i>	FWMSH93B.0 0026	-	-	19	0.243	1.491	Paulina-Carabajal et al. (2016)
<i>Tyrannosaurus rex</i>	AMNH FR 5117	-	-	13.8	0.579	2.109	Witmer and Ridgely (2009)
<i>Gorgosaurus libratus</i>	ROM 1247	-	-	8.15	1.484	3.778	Witmer and Ridgely (2009)
<i>Allosaurus fragilis</i>	UMNH VP 18050	-	-	14.8	0.49	1.945	Witmer and Ridgely (2009)
“ <i>Troodon formosus</i> ”	composite of TMP 86.36.457 and TMP 79.8.1	-	-	9.56	1.173	3.205	Witmer and Ridgely (2009)

Relative ASC height, height of the anterior semicircular canal/external diameter of anterior semicircular canal; Relative PSC height, height from the base of the posterior semicircular canal to the plane of the lateral semicircular canal/height of the posterior semicircular canal. “Best frequency of hearing” and “High frequency hearing limit” were calculated following the method of Gleich et al. (2005).

on the endocast in *P. lujiatunensis* (Zhou et al., 2007), in contrast to the situation in *P. amitabha* (Napoli et al., 2019). The cerebellar flocculus (floccular lobe) extends laterally to cross the plane defined by the ASC in both specimens. It is not visible on the endocast of neoceratopsians such as

Protoceratops, *Pachyrhinosaurus*, *Anchiceratops*, and *Triceratops* (Brown, 1914; Hopson, 1979; Forster, 1996; Witmer et al., 2008). Its presence on the endocast of *Psittacosaurus* has not been recognized in earlier studies (Zhou et al., 2007; Napoli et al., 2019), but differences

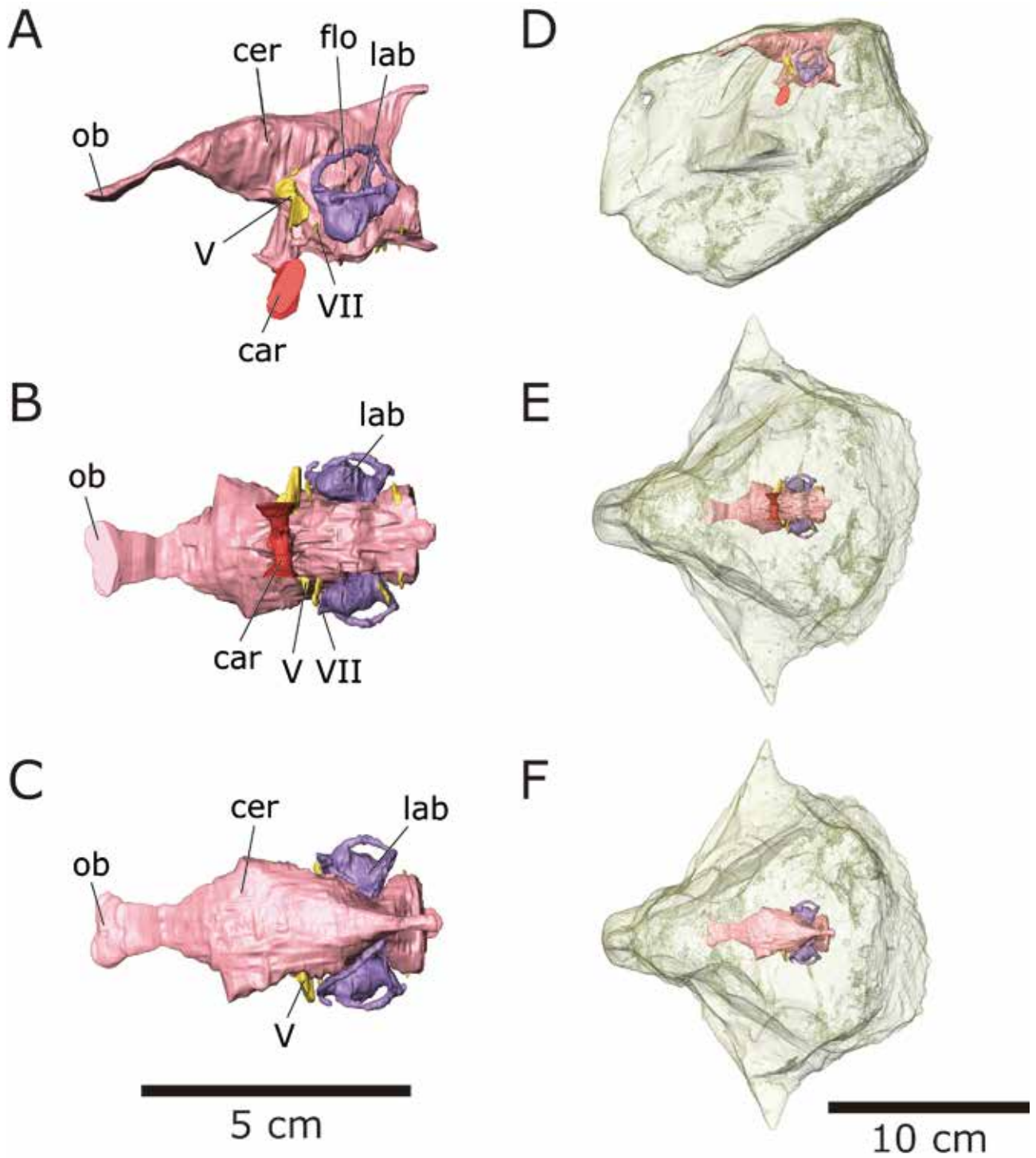


Figure 2. Cranial endocast (A–C) and skull (D–F) of ZMNH M12414 in left lateral (A, D), ventral (B, E), and dorsal (C, F) views. Cranial endocast, cranial nerves, carotid artery, and endosseous labyrinths are represented by pink, yellow, red, and purple colorings, respectively. Abbreviations: car, carotid artery; cer, cerebral hemisphere; flo, cerebellar flocculus; lab, labyrinth; ob, olfactory bulb; V, trigeminal nerve; VII, facial nerve; VII, vestibulocochlear nerve; IX–XI, shared canal for glossopharyngeal, vagus, and accessory nerves; XII-1, first branch of hypoglossal nerve; XII-2, second branch of hypoglossal nerve.

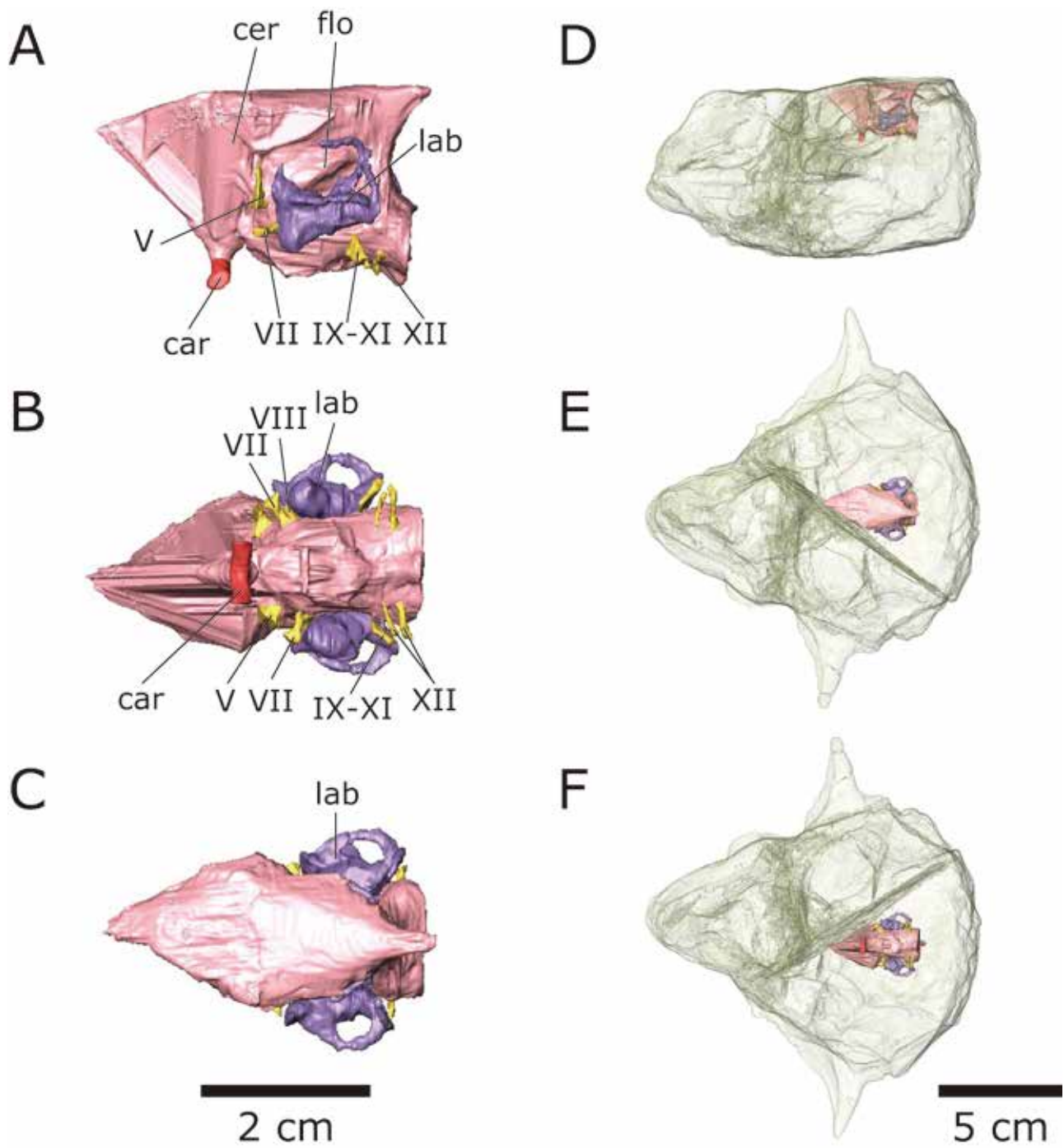


FIGURE 3. Cranial endocast (A–C) and braincase (D–F) of ZMNH M12423 in left lateral (A, D), ventral (B, E), and dorsal (C, F) views. Color scheme and abbreviations as in Fig. 2.

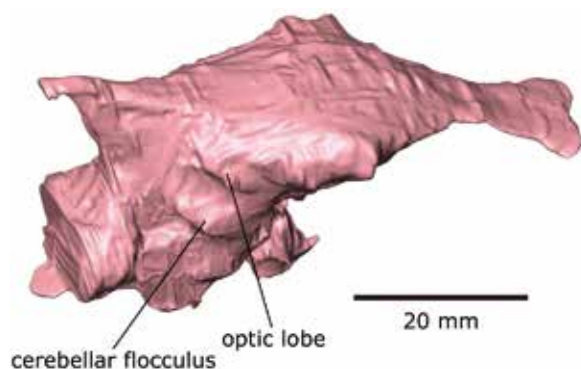


FIGURE 4. Optic lobe and cerebellar flocculus of ZMNH M12414 in right lateral view. Only the cranial endocast is shown for clarity.

regarding the preservation of the specimens or the CT image resolution may have allowed the identification of optic lobes in this study.

Only the internal carotid arteries could be reconstructed from the vascular system in both specimens. The internal carotid arteries extend lateroventrally from the ventral end of the pituitary (Figs. 2 and 3).

Cranial nerves

The cranial endocast includes the roots of some cranial nerves (CNs) and the accompanying assemblage of soft tissues, such as blood vessels. However, because the latter is difficult to discern independently in endocasts, we will focus on the morphology of the cranial nerves here.

The canals for the optic, oculomotor, trochlear, and abducens nerves (CNs II–IV, VI) are not visible in the specimens due to preservation. In lateral view, the canal for the trigeminal nerve (CN V) projects anterolaterally from the area posteroventral to the cerebrum at the level of the LSC of the inner ear. This nerve exits through one opening on the laterosphenoid-prootic suture. In ZMNH M12423, the canal for the facial nerve (CN VII) that extends anterolaterally to exit through the prootic is preserved. The canal for the vestibulocochlear nerve (CN VIII) extends from just posterior to the facial nerve canal laterally to connect with the vestibule of the inner ear. The canal for the glossopharyngeal vagus, and accessory nerves (CNs IX–XI) is also observed as a single trunk. This structure is known in many amniotes and is typically called the vagal canal (Sampson and Witmer 2007; Witmer et al. 2008). The vagal canal extends posteroventrally to open in the otoccipital in ZMNH M12423. The two canals for the hypoglossal nerves (CN XII) are positioned posterior to the vagal canal and extend posterolaterally.

Endosseous labyrinth

The labyrinths of the inner ear are preserved on both sides of ZMNH M12414 (Figs. 2, 5) and ZMNH M12423 (Figs. 3, 6) but cannot be fully reconstructed in ZMNH M12423 in which the ASC is only partially discernible in the CT images, possibly due to poor preservation. The inner ear is located posterolateral to the cerebellum. The ASC is dorsoventrally taller than the PSC, contrary to the conditions in *Anchiceratops*, *Pachyrhinosaurus lakustai*, *Pachyrhinosaurus perotorum*, and *Triceratops* sp. (Brown 1914; Witmer and Ridgely 2008; Tykoski and Fiorillo 2013; Sakagami and Kawabe 2020) in which they have roughly the same height. In this regard, the ASC of *P. lujiatunensis* is more reminiscent of the situation in theropods such as *Tyrannosaurus* (Witmer and Ridgely 2009). In lateral view, when the LSC is oriented horizontally, the ASC curves unevenly from its dorsal extremity to the anterior tip of the LSC, and the PSC extends ventrally slightly beyond the level of the LSC. The cochlear duct is 5.07 mm tall dorsoventrally on the left side of ZMNH M12414 and 4.33 mm on the left side of ZMNH M12423. Based on these lengths, the best frequency of hearing is estimated to be 2479 Hz for ZMNH M12414 and 2804 Hz for ZMNH M12423 (Table 2). The quotient of dividing the height by the external diameter of the ASC is 1.353 in ZMNH M12414 and 1.381 in ZMNH M12423 (Table 2). The quotient of dividing the total height of the PSC by the portion of it that extends ventrally beyond the LSC plane is 0.416 in ZMNH M12414 and 0.428 in ZMNH M12423 (Table 2). In lateral view, the angle between the palatal plane and the LSC plane is about 15° and 5° in ZMNH M12414 and M12423, respectively.

DISCUSSION

Head posture

The LSC provides valuable information for estimating the head posture of extinct animals since the alert head postures of extinct animals can be somewhat deduced from positioning the LSC horizontally (Duijm 1951). In this study, the angles between the plane of the LSC and the palatal plane were measured and considered as the head posture. The results showed that ZMNH M 12414 had a palatal plane tilted 15° ventrally from the horizontal plane (Fig. 7). Bullar et al. (2019) estimated the head posture of three *Psittacosaurus lujiatunensis* at different developmental stages. They found that a hatchling individual (IVPP V15451), estimated to be less than one year old, had a 38° head posture, a juvenile individual (IVPP V22647), estimated to be approximately two years old, had a 25° posture, and a 10-year-old adult (IVPP V12617) was tilted 15°. The head posture of ZMNH M12414, which is estimated to be roughly adult at six years of age, at 15°, is consistent with the results shown by Bullar et al. (2019) for IVPP V12617.

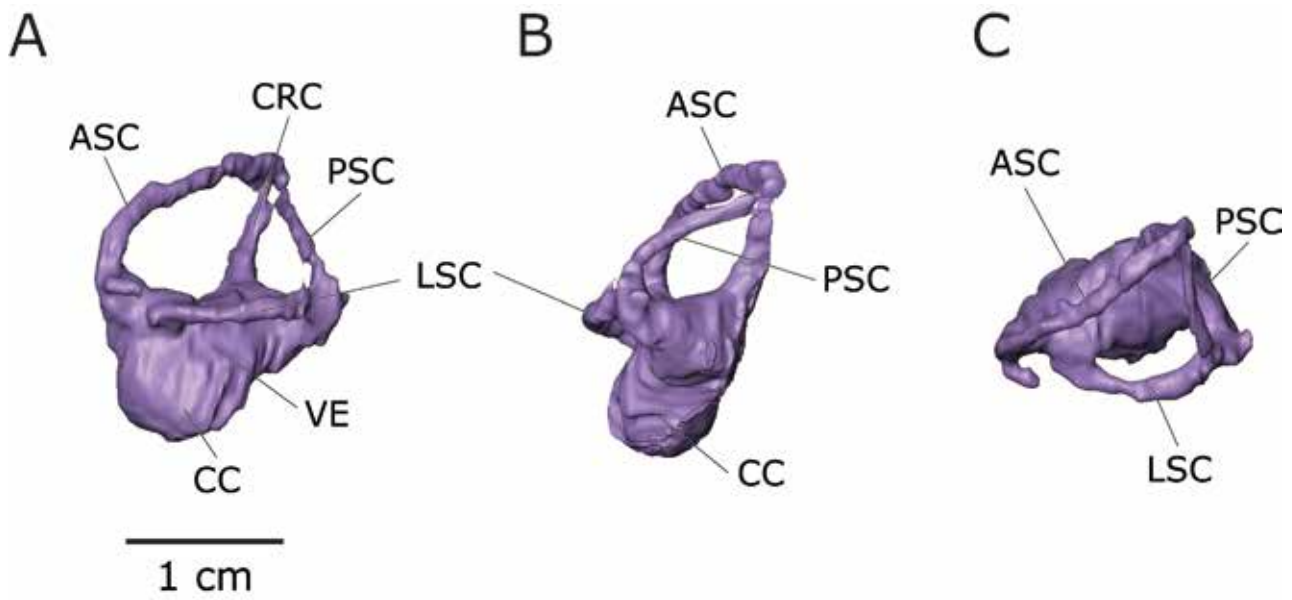


FIGURE 5. Left endosseous labyrinth of ZMNH M12414 in lateral (A), posterior (B), and dorsal (C) views. Abbreviations: ASC, anterior semicircular canal; CC, cochlea; CRC, crus commune; LSC, lateral semicircular canal; PSC, posterior semicircular canal; VE, vestibule of inner ear.

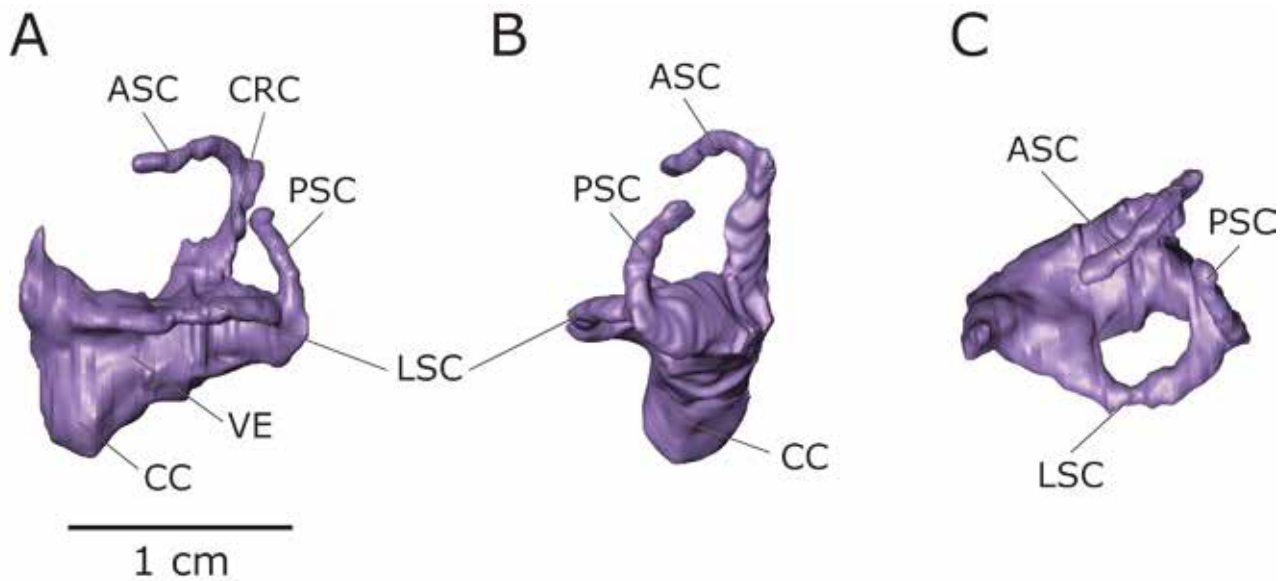


FIGURE 6. Left endosseous labyrinth of ZMNH M12423 in lateral (A), posterior (B), and dorsal (C) views. Abbreviations as in Fig. 5.

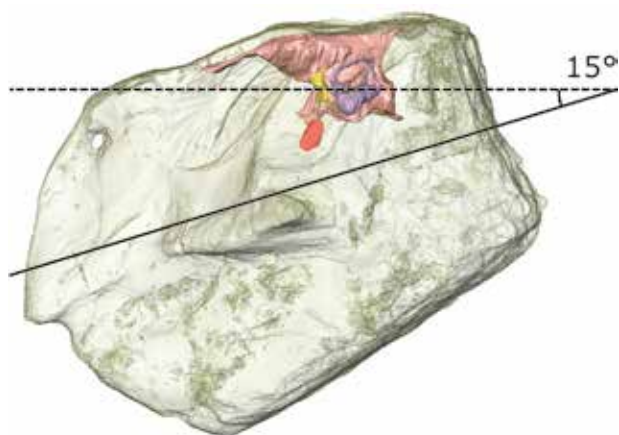


FIGURE 7. The possible head posture of *Psittacosaurus* (ZMNH M12414) when the lateral semicircular canal is Earth horizontal. The solid and broken lines indicate the palatal plane and the plane of the lateral semicircular canal, respectively.

On the other hand, the head posture of ZMNH M12423, estimated to be roughly adult at four years of age, is suggested as only 5° below the horizontal plane. Considering the results of Bullar et al. (2019), the head posture of ZMNH M12423 would be expected to be between 15° and 25°, but the values obtained in this study deviate significantly from this range. This may be due to the deformation of the rostrum, which is bent dorsally to the neurocranium. However, the degree of deformation of ZMNH M12423 is not extreme, and even in the absence of deformation, the head posture would not appear to be as angled as described by Bullar et al. (2019). Change in head posture during the development of *P. lujiatunensis* would become clearer with the study of well-preserved specimens.

It should be noted that a certain degree of error in the LSC-based head posture reconstruction has been reported successively in recent years (Marugán-Lobón et al. 2013; Berlin et al. 2013; Coutier et al. 2017). Although more detailed discussion is needed to determine whether this angle accurately reflects the posture of *P. lujiatunensis* in its natural habitat, it is still meaningful to use the LSC as a standard for intraspecific comparison of head postures, and it is valuable for understanding how the head posture of *P. lujiatunensis* changed during development.

Stabilization of gaze and posture

The enlarged cerebellar flocculi observed in this study are a unique feature found only in *P. lujiatunensis* and not in any other ceratopsians (Brown 1914; Hopson 1979; Zhou et al. 2007; Witmer and Ridgely 2008; Tykoski and Fiorillo 2013). Such enlarged cerebellar flocculi are also known in extant

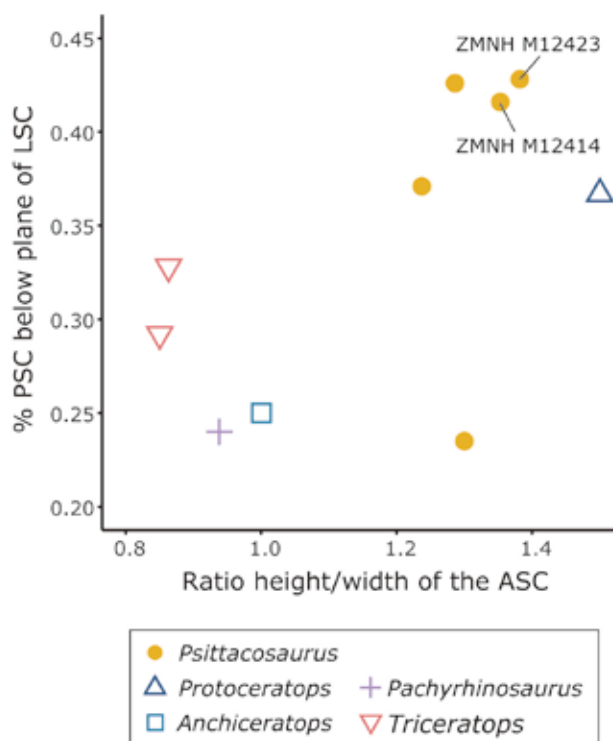


FIGURE 8. Comparative proportions of ASC and PSC. Scatterplots of the percentage of the PSC situated inferiorly to the plane of the LSC versus ratio height/width of the ASC in ceratopsians.

birds, non-avian theropods, and pterosaurs (Witmer et al. 2003; Witmer and Ridgely 2009; Walsh et al. 2013; Ballell et al. 2021). Witmer et al. (2003) argued that the size of the cerebellar flocculus (relative to total brain mass) is linked to the ability to stabilize gaze. Hence, Witmer et al. (2003) assumed that pterosaurs possibly had better gaze stabilization due to their enlarged cerebellar flocculi. On the other hand, Walsh et al. (2013) found no significant relationship between the relative size of the flocculus (floccular fossa volume relative to endocranial volume) and flight mode classification in extant birds and concluded that the floccular fossa size is not a proxy for flying control. Walsh et al. (2013) also found that obligate terrestrial birds such as emus had slightly larger flocculi than flying birds – possibly due to the unstable nature of bipedal locomotion. Walsh et al. (2013) also suggest that the enlarged flocculi observed in non-avian dinosaurs and pterosaurs are possibly related to the evolution of bipedal terrestrial locomotion because it requires better gaze stability than quadrupedal locomotion. In the case of *P. lujiatunensis*, the enlargement of the cerebellar flocculi, in combination with the well-developed semicircular canals (discussed below), may suggest that psittacosaurus possessed a better sense of gaze stabilization than other ceratopsians.

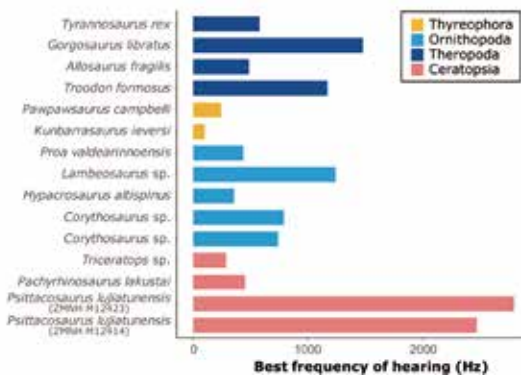


FIGURE 9. Best frequency of hearing for selected dinosaurs.

The relationships between the morphology of the semicircular canals and the sense of balance, the agility of locomotion, and the stabilization of gaze have been discussed (e.g., Spoor et al. 2007). In order to assess the degree of semicircular-canal development of an avialan theropod, *Archaeopteryx*, Domínguez Alonso et al. (2004) investigated the ratios between the height and external diameter of the ASC and the percentage of the height of the PSC that extends below the plane of the LSC. The present study compared these ratios with those of ceratopsians (Table 3). These ratios for ZMNH M12414 and M12423 were added to the dataset of Sakagami and Kawabe (2020) (Fig. 8). ZMNH M12414 and M12423 plot in the region showing a relatively tall ASC and a ventrally projecting PSC. This is consistent with Sakagami and Kawabe's (2020) results, in which basal ceratopsians, including *P. lujiatunensis*, had well-developed ASC and greater gaze stability than derived ones.

Hearing ability

In extant animals – including mammals, birds, and reptiles – the CL has been used as an indicator of hearing ability because the length of the basilar papilla within the cochlear duct is correlated with hearing frequency (see Walsh et al. 2009). Similarly, the CL has been used to estimate the hearing ability of extinct animals including dinosaurs (Evans et al. 2009). In this study, we added the data of two specimens of *P. lujiatunensis* into Sakagami and Kawabe's (2020) dataset and compared them with the hearing frequency of a sample of dinosaurs (Fig. 9). When compared with other non-avian dinosaurs, the best frequency of hearing for *P. lujiatunensis* is relatively high. However, it must be noted that CL values for ZMNH M12414 and M12423 were well outside the ranges of those employed to empirically derive the regression equation in Gleich et al. (2005), which may lead to erroneous estimation of the best frequency of hearing.

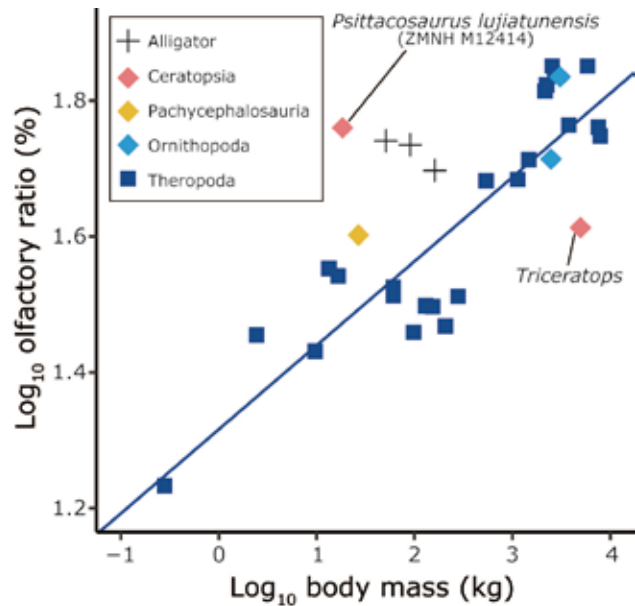


FIGURE 10. Scatterplot of olfactory ratio versus body mass for alligators, ceratopsids, a pachycephalosaurid, ornithopods, and theropods. The line is the least-squares linear regression line ($y = 0.1237x + 1.316$) for theropods as calculated by Zelenitsky et al. (2009).

Olfactory bulbs and sense of smell

The relative degree of development of the olfactory bulb is supposed to indicate the acuity of the sense of smell in extant mammals and archosaurs based on a positive correlation between the olfactory bulb size and olfactory acuity (Cobb 1960; Zelenitsky et al. 2009). The olfactory ratio of ZMNH M12414 is compared with those of theropods, other dinosaurs, and alligators in a scatter plot of log10 olfactory ratio against log10 body mass provided by Zelenitsky et al. (2009) and Sakagami and Kawabe (2020). ZMNH M12414 plots considerably above the regression line (Fig. 10), indicating that the acuity of the sense of smell of *P. lujiatunensis* was higher than the average of the taxa considered in the analysis. Our results are consistent with the observations by Zhou et al. (2007), according to which *P. lujiatunensis* has an enlarged olfactory bulb. In contrast to *P. lujiatunensis*, late-diverging ceratopsians (*Pachyrhinosaurus* and *Triceratops*) are regarded as exhibiting relatively small olfactory bulbs (Witmer and Ridgely 2008; Sakagami and Kawabe 2020). The present study quantitatively demonstrates that *P. lujiatunensis* has a relatively large olfactory bulb, which supports a more acute sense of smell than in derived ceratopsians.

CONCLUSIONS

In this study, cranial endocasts of *Psittacosaurus*

lujiatunensis were reconstructed by CT analyses of two new specimens. Our examination revealed enlarged cerebellar flocculi, which have not been reported in any other ceratopsian. The enlarged cerebellar flocculi imply better gaze stability. This observation is consistent with the morphometry of the semicircular canals, in which the ASC is relatively tall and the PSC projects more ventrally. Furthermore, the orientation of the LSC and the relatively large olfactory bulb indicate a slightly downward head posture and a relatively acute sense of smell, respectively. In addition, the best frequency of hearing of two specimens of *P. lujiatunensis* based on the cochlear length were 2479 and 2804 Hz, which may have been relatively high when compared to other dinosaurs.

Thanks to high-resolution CT analyses, this study substantially informs the study of the ecology and habits of *P. lujiatunensis*. Furthermore, it demonstrates that the development of CT techniques enables re-assessment of the neuroanatomy in fossil taxa and helps collect more data in quality and quantity, leading to a better understanding of the biology of said taxa.

ACKNOWLEDGEMENTS

We thank the College of Civil Engineering and Architecture, Zhejiang University staff for assisting in conducting CT analyses and the researchers and staff of the Zhejiang Museum of Natural History and Fukui Prefectural Dinosaur Museum for providing information about the specimens. The Institute of Dinosaur Research, Fukui Prefectural University members provided helpful comments and suggestions for this study. Dr. Fabien Knoll (ARAIDFundación Conjunto Paleontológico de Teruel-Dinópolis) and Dr. Qi Zhao (Key Laboratory of Vertebrate Evolution and Human Origins, Institute of Vertebrate Paleontology and Paleoanthropology, Chinese Academy of Sciences) provided helpful reviews. The authors also thank Takuya Imai (Institute of Dinosaur Research of Fukui Prefectural University) for the English language review. This work was supported by JSPS KAKENHI Grant Number 21K03737.

REFERENCES

- Balanoff, A. M., G. S. Bever, M. W. Colbert, J. A. Clarke, D. J. Field, P. M. Gignac, D. T. Ksepka, R. C. Ridgely, N. A. Smith, C. R. Torres, S. Walsh and L. M. Witmer. 2016. Best practices for digitally constructing endocranial casts: examples from birds and their dinosaurian relatives. *Journal of Anatomy* 229: 173–190.
- Ballell, A., J. L. King, J. M. Neenan, E. J. Rayfield and M. J. Benton. 2021. The braincase, brain and palaeobiology of the basal sauropodomorph dinosaur *Thecodontosaurus antiquus*. *Zoological Journal of the Linnean Society* 193: 541–562.
- Berlin, J. C., E. C. Kirk and T. B. Rowe. 2013. Functional implications of ubiquitous semicircular canal non-orthogonality in mammals. *PLOS ONE* 8: 24–26.
- Brown, B. 1914. *Anchiceratops*, a new genus of horned dinosaurs from the Edmonton Cretaceous of Alberta; with Discussion of the origin of the ceratopsian crest and the brain casts of *Anchiceratops* and *Trachodon*. *Bulletin American Museum of Natural History* 33: 539–548.
- Bullar, C. M., Q. Zhao, M. J. Benton and M. J. Ryan. 2019. Ontogenetic braincase development in *Psittacosaurus lujiatunensis* (Dinosauria: Ceratopsia) using microcomputed tomography. *PeerJ* 7: e7217.
- Cobb, S. 1960. A Note on the Size of the Avian Olfactory Bulb. *Epilepsia* 1: 394–402.
- Corfield, J. R., J. M. Wild, B. R. Cowan, S. Parsons and M. F. Kubke. 2008. MRI of postmortem specimens of endangered species for comparative brain anatomy. *Nature Protocols* 3: 597–605.
- Coutier, F., L. Hautier, R. Cornette, E. Amson and G. Billet. 2017. Orientation of the lateral semicircular canal in Xenarthra and its links with head posture and phylogeny. *Journal of Morphology* 278:704–717.
- Domínguez Alonzo, P., A. C. Milner, R. A. Ketcham, M. J. Cookson and T. B. Rowe. 2004. The avian nature of the brain and inner ear of *Archaeopteryx*. *Nature* 430: 666–669.
- Duijm, M. 1951. On the head posture of some birds and its relation to some anatomical features. *Proceedings of the Koninklijke Nederlandse Akademie van Wetenschappen* 54: 260–271.
- Erickson, G. M., P. J. Makovicky, B. D. Inouye, C. F. Zhou and K.-Q. Gao. 2009. A life table for *Psittacosaurus lujiatunensis*: Initial insights into ornithischian dinosaur population biology. *Anatomical Record* 292: 1514–1521.
- Evans, D. C., R. Ridgely and L. M. Witmer. 2009. Endocranial anatomy of lambeosaurine hadrosaurids (Dinosauria: Ornithischia): A sensorineural perspective on cranial crest function. *Anatomical Record* 292: 1315–1337.
- Forster, C. A. 1996. New information on the skull of *Triceratops*. *Journal of Vertebrate Paleontology* 16: 246–258.
- Gleich, O., R. J. Dooling and G. A. Manley. 2005. Audiogram, body mass, and basilar papilla length: Correlations in birds and predictions for extinct archosaurs. *Naturwissenschaften* 92: 595–598.
- Hedrick, B. P., and P. Dodson. 2013. Lujiatun Psittacosaurids: Understanding Individual and Taphonomic Variation Using 3D Geometric Morphometrics. *PLOS ONE* 8: e69265.
- Hopson, J. A. 1979. Paleoneurology; pp. 39–146 in C. Gans, R. G. Northcutt and P. Ulinski (eds.), *Biology of the Reptilia*. 9. Academic Press, London.
- Jirak, D., and J. Janacek. 2017. Volume of the crocodylian brain and endocast during ontogeny. *PLOS ONE* 12: e0178491.
- Knoll, F., S. Lautenschlager, S. Kawabe, G. Martínez, E. Espílez, L. Mampel and L. Alcalá. 2021. Palaeoneurology of the Early Cretaceous iguanodont *Proa valdearinnoensis* and its bearing on the parallel developments of cognitive abilities in theropod and ornithomimid dinosaurs. *Journal of Comparative Neurology*, 529: 3922–3945.

- Langston Jr., W. 1975. The Ceratopsian Dinosaurs and Associated Lower Vertebrates from the St. Mary River Formation (Maestrichtian) at Scabby Butte, Southern Alberta. *Canadian Journal of Earth Sciences* 12: 1576–1608.
- Leahey, L. G., R. E. Molnar, K. Carpenter, L. M. Witmer and S. W. Salisbury. 2015. Cranial osteology of the ankylosaurian dinosaur formerly known as *Minmi* sp. (Ornithischia: Thyreophora) from the Lower Cretaceous Allaru Mudstone of Richmond, Queensland, Australia. *PeerJ* 3: e1475.
- Li, Y., B. R. Jicha, Z. Yu, H. Wu, X. Wang, B. S. Singer, H. He and Z. Zhou. 2022. Rapid preservation of Jehol Biota in Northeast China from high precision $40\text{Ar}/39\text{Ar}$ geochronology. *Earth and Planetary Science Letters* 594: 117718.
- Marugán-Lobón, J., L. M. Chiappe, and A. A. Farke. 2013. The variability of inner ear orientation in saurischian dinosaurs: testing the use of semicircular canals as a reference system for comparative anatomy. *PeerJ* 1: e124.
- Napoli, J. G., T. Hunt, G. M. Erickson and M. A. Norell. 2019. *Psittacosaurus amitabha*, a new species of ceratopsian dinosaur from the Ondai Sayr Locality, Central Mongolia. *American Museum Novitates* 3932: 1–36.
- Paulina-Carabajal, A., Y. N. Lee and L. L. Jacobs. 2016. Endocranial morphology of the primitive nodosaurid dinosaur *Pawpawsaurus campbelli* from the Early Cretaceous of North America. *PLOS ONE* 11: e0150845
- Sakagami, R., and S. Kawabe. 2020. Endocranial anatomy of the ceratopsid dinosaur *Triceratops* and interpretations of sensory and motor function. *PeerJ* 8: e9888.
- Sampson, S. D., and L. M. Witmer. 2007. Craniofacial anatomy of *Majungasaurus crenatissimus* (Theropoda: Abelisauridae) from the late cretaceous of madagascar. *Journal of Vertebrate Paleontology* 27: 32–104.
- Spoor, F., T. Garland, G. Krovitz, T. M. Ryan, M. T. Silcox and A. Walker. 2007. The primate semicircular canal system and locomotion. *Proceedings of the National Academy of Sciences of the United States of America* 104: 10808–10812.
- Spoor, F., and F. Zonneveld. 1998. Comparative review of the human bony labyrinth. *Yearbook of Physical Anthropology* 41: 211–251.
- Tykoski, R. S., and A. R. Fiorillo. 2013. Beauty or brains? The braincase of *Pachyrhinosaurus perotorum* and its utility for species-level distinction in the centrosaurine ceratopsid *Pachyrhinosaurus*. *Earth and Environmental Science Transactions of the Royal Society of Edinburgh* 103: 487–499.
- Walsh, S. A., P. M. Barrett, A. C. Milner, G. Manley and L. M. Witmer. 2009. Inner ear anatomy is a proxy for deducing auditory capability and behaviour in reptiles and birds. *Proceedings of the Royal Society B: Biological Sciences* 276: 1355–1360.
- Walsh, S. A., A. N. Iwaniuk, M. A. Knoll, E. Bourdon, P. M. Barrett, A. C. Milner, R. L. Nudds, R. L. Abel and P. Dello Sterpaio. 2013. Avian cerebellar floccular fossa size is not a proxy for flying ability in birds. *PLOS ONE* 8: e67176.
- Watanabe, A., P. M. Gignac, A. M. Balanoff, T. L. Green, N. J. Kley and M. A. Norell. 2019. Are endocasts good proxies for brain size and shape in archosaurs throughout ontogeny? *Journal of Anatomy* 234: 291–305.
- Witmer, L. M., S. Chatterjee, J. Franzosa and T. Rowe. 2003. Neuroanatomy of flying reptiles and implications for flight, posture and behaviour. *Nature* 425: 950–953.
- Witmer, L. M., and Ridgely R. C. 2008. Structure of the brain cavity and inner ear of the centrosaurine ceratopsid dinosaur *Pachyrhinosaurus* based on CT scanning and 3D visualization; pp. 117–144 in P. J. Currie, W. Langstone Jr. and D. H. Tanke (eds.), *A new horned dinosaur from an Upper Cretaceous bone bed in Alberta*. National Research Council of Canada Monograph Series, Ottawa.
- Witmer, L. M., and R. C. Ridgely. 2009. New insights into the brain, braincase, and ear region of tyrannosaurs (Dinosauria, Theropoda), with implications for sensory organization and behavior. *The Anatomical Record: Advances in Integrative Anatomy and Evolutionary Biology* 292: 1266–1296.
- Witmer, L. M., R. C. Ridgely., D. L. Dufeu and M. C. Semones. 2008. Using CT to Peer into the Past: 3D Visualization of the Brain and Ear Regions of Birds, Crocodiles, and Nonavian Dinosaurs; pp. 67–87 in H. Endo and R. Frey (eds.), *Anatomical Imaging: Towards a New Morphology*. Springer Japan, Tokyo.
- Zelenitsky, D. K., F. Therrien and Y. Kobayashi. 2009. Olfactory acuity in theropods: palaeobiological and evolutionary implications. *Proceedings of the Royal Society B: Biological Sciences* 276:667–673.
- Zhang, Q. N., J. L. King, D. Q. Li, Y. M. Hou and H. L. You. 2020. Endocranial morphology of *Auroraceratops* sp. (Dinosauria: Ceratopsia) from the Early Cretaceous of Gansu Province, China. *Historical Biology* 32: 1355–1360.
- Zhao, Q., M. J. Benton, X. Xu and P. M. Sander. 2014. Juvenile-only clusters and behaviour of the early Cretaceous Dinosaur *Psittacosaurus*. *Acta Palaeontologica Polonica* 59: 827–833.
- Zhou, C. F., K.-Q. Gao, R. C. Fox and X. K. Du. 2007. Endocranial morphology of psittacosaurus (Dinosauria: Ceratopsia) based on CT scans of new fossils from the Lower Cretaceous, China. *Palaeoworld* 16: 285–293.